Noise on the non-Abelian $\nu = 5/2$ Fractional Quantum Hall Edge

Jinhong Park,[1,2,*] Christian Spånslätt,[3,4,†] Yuval Gefen,[2,3] and Alexander D. Mirlin[3,4,5,6]

[1]*Institute for Theoretical Physics, University of Cologne, Zülpicher Strasse 77, 50937 Köln, Germany*
[2]*Department of Condensed Matter Physics, Weizmann Institute of Science, Rehovot 76100, Israel*
[3]*Institute for Quantum Materials and Technologies, Karlsruhe Institute of Technology, 76021 Karlsruhe, Germany*
[4]*Institut für Theorie der Kondensierten Materie, Karlsruhe Institute of Technology, 76128 Karlsruhe, Germany*
[5]*Petersburg Nuclear Physics Institute, 188300 St. Petersburg, Russia*
[6]*L. D. Landau Institute for Theoretical Physics RAS, 119334 Moscow, Russia*

(Received 10 June 2020; accepted 10 September 2020; published 9 October 2020)

The recent measurement of a half-integer thermal conductance for the $\nu = 5/2$ fractional quantum Hall state has confirmed its non-Abelian nature, making the question of the underlying topological order highly intriguing. We analyze the shot noise at the edge of the three most prominent non-Abelian candidate states. We show that the noise scaling with respect to the edge length can, in combination with the thermal conductance, be used to experimentally distinguish between the Pfaffian, anti-Pfaffian, and particle-hole-Pfaffian edge structures.

DOI: 10.1103/PhysRevLett.125.157702

Introduction.—The fractional quantum Hall (FQH) [1,2] state at filling $\nu = 5/2$ [3] is the prototypical candidate for a phase of matter with non-Abelian topological order [4]. Such order has attracted immense attention during the last decades, not least for its remarkably rich theoretical structure [5], but also as a promising platform for topological quantum computation [6].

The $5/2$ state is believed to consist of two filled lowest Landau levels (LLLs) with opposite spin polarizations and one half filled and spin polarized second Landau level (2LL) [7–13]. For this structure, a wide variety of theoretical candidate states have been proposed, among which the most prominent are the Pfaffian (PF) [4], anti-Pfaffian (APF) [14,15], and particle-hole Pfaffian (PHPF) [16–19], all exhibiting non-Abelian order. Also, several Abelian states have been proposed [20–23]. To date, numerical simulations seem to favor the APF state [7,24,25], while tunneling experiments point either toward the APF, $SU(2)_2$, 331, or 113 states [26–28]. All proposed candidates are compatible with the Hall conductance $G_H = 5e^2/2h$, but they differ in their bulk topological order, manifested by different edge structures [29–31] [see Fig. 1(a)]. A fruitful route in determining the nature of the $5/2$ state is therefore by thermal edge transport experiments [32–35]. If the edge fully equilibrates due to efficient interchannel tunneling, the thermal Hall G_H^Q and two-terminal G^Q conductances are quantized as

$$G_H^Q = \nu_Q \kappa T, \qquad G^Q = |G_H^Q|, \tag{1}$$

where $\kappa = \pi^2 k_B^2/3h$, T is the temperature, and k_B is the Boltzmann constant. The topological quantity $\nu_Q \equiv c - \bar{c}$ is the difference in the central charges of the chiral (c) and the antichiral ($\bar{c}$) sectors of the edge conformal field theory [36,37]. With insufficient equilibration, $G^Q/\kappa T$ may, however, take any value between $c + \bar{c}$ and $|\nu_Q|$. For an Abelian edge, c and $\bar{c}$ coincide with the number of downstream (the chirality direction set by the magnetic field) and upstream (opposite direction to downstream) edge channels, respectively [36,37]. By contrast, a chiral Majorana edge mode ψ, present only on non-Abelian edges, contributes instead with $c_\psi = 1/2$, implying a half-integer quantization in Eq. (1). Indeed, Banerjee *et al.* [34] recently found $G^Q/\kappa T \approx 5/2$, a clear signature of non-Abelian order. This particular value of G^Q was further interpreted as favoring the PHPF state for which $\nu_Q = 5/2$. The PHPF edge structure can also be obtained in models with random puddles of alternating non-Abelian orders [38–43]. At the same time, theories of partial equilibration have been put forward, allowing the APF edge to remain a viable candidate [44–48]. To our knowledge, no reconciliation between experiment and theory for the pure PF edge, where $G_H^Q/\kappa T = 7/2$ regardless of equilibration, has so far been made. Hence, the question whether the $\nu = 5/2$ state displays APF or PHPF topological order remains open and pressing.

In this Letter, we propose that shot noise [49,50] measurements are a powerful tool to distinguish between all three non-Abelian $5/2$ candidate states [see Fig. 1(b)]. We show that in the transport regime with complete edge equilibration, which requires strong Landau level mixing (LLM), the dc noise S either vanishes or decreases exponentially with increasing edge length L. However, in the transport regime where LLM is negligible but equilibration within the 2LL is efficient, the APF edge uniquely exhibits the scaling $S \simeq c_1 - c_2\sqrt{L/\ell_{\rm eq}}$ with

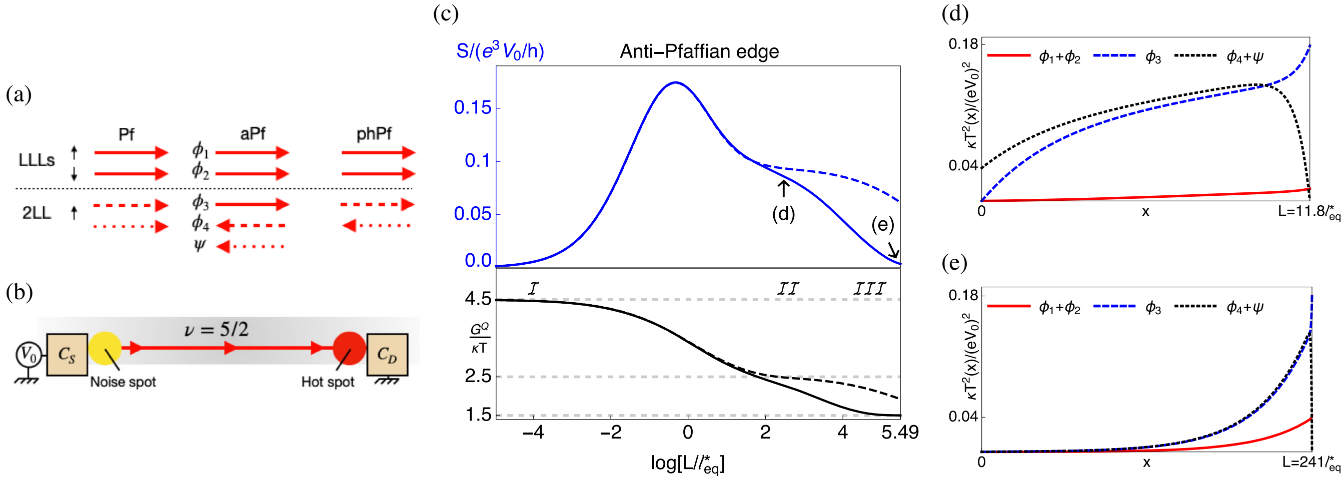

FIG. 1. (a) LLL and 2LL edge structures of PF, APF, and PHPF states. Thick lines: unit-charge bosonic channels; dashed lines: charge $1/2$ bosons; dotted lines: Majorana channels. Arrows denote downstream (right-pointing) or upstream (left-pointing) propagation. Black arrows indicate spin. (b) Schematic setup for measuring the noise S. The contacts are separated by distance L; one of them is biased with V_0. In the equilibrated regime, heat is generated at the hot spot (red dot), while noise is generated due to partitioning of electron-hole pairs at the noise spot (yellow dot). (c) Shot noise $S/(V_0 e^3/h)$ and thermal conductance $G^Q/\kappa T$ of the APF edge as functions of $\log[L/\ell^*_{\rm eq}]$ for $\ell_{\rm eq} = 100$ (solid lines) and $\ell_{\rm eq} = 1000$ (dashed lines). In regime $\mathcal{I}$ (see Table I) equilibration and S are weak and $G^Q/\kappa T = 9/2$. In regime $\mathcal{II}$ (weak LLM, but efficient intra-2LL equilibration), S is approximately constant and $G^Q/\kappa T \approx 5/2$. In regime $\mathcal{III}$ (full equilibration), S is exponentially suppressed and $G^Q/\kappa T \to 3/2$. (d) APF edge channel temperature profiles in regime $\mathcal{II}$ with $\ell_{\rm eq}/\ell^*_{\rm eq} = 100$ and $L \approx 11.8\ell^*_{\rm eq}$. Heat from the hot spot ($L - \ell^*_{\rm eq} \lesssim x \lesssim L$) reaches the noise spot ($0 \lesssim x \lesssim \ell^*_{\rm eq}$). (e) APF edge channel temperature profiles in regime $\mathcal{III}$ with $\ell_{\rm eq}/\ell^*_{\rm eq} = 100$ and $L \approx 241\ell^*_{\rm eq}$. The heat reaching the noise spot is exponentially small in L.

constants $c_1, c_2 > 0$ [see Fig. 1(c)]. Most interestingly, it is precisely in this semiequilibrated regime that $G^Q/\kappa T = 5/2$ for both the APF and PHPF states. It follows that, in combination with measurements of G^Q, the scaling of S with L uniquely distinguishes between the APF and PHPF edges.

These disparate scalings follow from a delicate interplay of charge and heat transport on the FQH edge. With strong equilibration, $L/\ell_{\rm eq} \gg 1$, where $\ell_{\rm eq}$ is a characteristic length [53] for charge and heat equilibration [54–57], noise is generated due to thermal partitioning of the charge current [58–60]. It is a remarkable consequence of the chiral edge nature that, when a current is driven between two contacts along an equilibrated FQH edge, heat is generated near the downstream contact (the hot spot), while noise is generated near the upstream contact (the noise spot) [see Fig. 1(b)]. Thus, noise generation requires a heat flow *upstream* from the hot spot to the noise spot, implying a deep connection between the noise characteristics and the nature of the heat transport along the edge. Since the latter is inherited from the bulk topological order, the topological significance of the noise scaling follows. For edges with $\nu_Q > 0$, $S \simeq 0$ (up to exponential corrections in $L/\ell_{\rm eq}$); for $\nu_Q = 0$, $S \simeq \sqrt{\ell_{\rm eq}/L}$ and for $\nu_Q < 0$, $S \simeq$ const. Hence, this noise classification constitutes a powerful probe for the FQH edge structure and provides a fully electrical method to detect upstream heat propagation.

To apply this classification to the three non-Abelian $\nu = 5/2$ edge candidates, we first define for each edge two length scales $\ell^*_{\rm eq}$ and $\ell_{\rm eq}$, which characterize intra-2LL and complete equilibration, respectively [61]. We assume $\ell^*_{\rm eq} \ll \ell_{\rm eq}$, which will be justified below. Next, we identify transport coefficients and noise scaling for the candidate edges in three transport regimes: $L \ll \ell^*_{\rm eq}$ (regime $\mathcal{I}$, clean regime), $\ell^*_{\rm eq} \ll L \ll \ell_{\rm eq}$ ($\mathcal{II}$, no LLM), and $\ell_{\rm eq} \ll L$ ($\mathcal{III}$, full equilibration) (see Table I). For the maximally chiral PF edge, no backscattering of charge or heat occurs.

TABLE I. Two-terminal electrical (G) and thermal (G^Q) conductances, and scaling of shot noise (S) with length L for PF, APF, and PHPF edges. Regime $\mathcal{I}$: no equilibration; regime $\mathcal{II}$: complete 2LL equilibration; regime $\mathcal{III}$: full equilibration. $S \simeq 0$ means exponentially small noise $S \sim e^{-L/\ell_{\rm eq}}$. Bold values: APF and PHPF edges show distinct noise scaling for the same G^Q.

	Transport characteristics	PF	APF	PHPF
$\mathcal{I}$	$G/(e^2/h)$	$5/2$	$7/2$	$5/2$
	$G^Q/(\kappa T)$	$7/2$	$9/2$	$7/2$
	S	0	$\propto L$	0
$\mathcal{II}$	$G/(e^2/h)$	$5/2$	$5/2$	$5/2$
	$G^Q/(\kappa T)$	$7/2$	$\mathbf{5/2}$	$\mathbf{5/2}$
	S	0	**const.**	**0**
$\mathcal{III}$	$G/(e^2/h)$	$5/2$	$5/2$	$5/2$
	$G^Q/(\kappa T)$	$7/2$	$3/2$	$5/2$
	S	0	$\simeq 0$	0

Thus, there is no charge partitioning and $S = 0$ in all regimes. Also, for the PHPF edge, charge propagates only downstream, hence no current partitioning and $S = 0$ in all regimes [62]. These results may be contrasted with the APF edge, which has a richer edge structure and is the focus of this Letter. In regime $\mathcal{I}$, we assume $S \propto L$ due to rare scattering events [58]. In regime $\mathcal{III}$, Eq. (1) gives $\nu_Q = 3/2$, which by our classification implies exponentially suppressed S. However, when the LLM is weak (regime $\mathcal{II}$), most of the noise is generated only in the 2LL due to a lack of backscattering in the two LLLs (which are to a large extent decoupled from the 2LL). The 2LL channels, within which heat flows upstream since $(c - \bar{c})|_{2\text{LL}} = -1/2$, lead to a constant noise $S \simeq c_1 - c_2\sqrt{L/\ell_{\text{eq}}}$ up to algebraic correction in L. This algebraic correction originates from the weak heat loss of the 2LLs to two LLLs. The existence of this noisy regime for the APF edge is our central observation. To investigate this regime, we next perform a detailed renormalization group (RG) analysis [55,66] of ℓ^*_{eq} and ℓ_{eq} for the APF edge.

Analysis of equilibration on the APF edge.—The APF edge consists of one left-moving charge neutral Majorana channel ψ (with velocity v_n) and four charged bosonic channels ϕ_i ($i = 1, \ldots, 4$), where ϕ_4 is left moving while the others are right movers [14,15] [see Fig. 1(a)]. The action is $S = S_0 + S_\psi$, with

$$S_0 = -\int dtdx \sum_{ij} \frac{1}{4\pi}[K_{ij}\partial_x\phi_i\partial_t\phi_j + V_{ij}\partial_x\phi_i\partial_x\phi_j],$$

$$S_\psi = \int dtdx[i\psi(\partial_t - v_n\partial_x)\psi]. \tag{2}$$

Here, the topological matrix $K = \text{diag}(1, 1, 1, -2)$ in the basis $(\phi_1, \phi_2, \phi_3, \phi_4)$, and the nonuniversal matrix V contains on its diagonal all bosonic velocities, while the off-diagonal elements describe interchannel repulsive interactions. We ignore density-density interactions involving ψ, since these are RG irrelevant at low temperatures. The action (2) is integrable and involves no mechanism for equilibration between the channels. In the absence of such a mechanism, we have $G/(e^2/h) = \sum_i |K^{-1}_{ii}| = 7/2$ and $G^Q/\kappa T = 4 + 1/2 = 9/2$. We can introduce equilibration by adding random interchannel electron tunneling [67]. Assuming that channels in the 2LL are spatially far away from the LLL channels, equilibration occurs dominantly within the 2LL [46]. We may then add the following random disorder perturbation [14]:

$$S_{2\text{LL}} = \int dtdx[\xi_{2\text{LL}}(x)\psi e^{i2\phi_4 + i\phi_3} + \text{H.c.}], \tag{3}$$

where $e^{i\phi_3}$ annihilates a right-moving electron, while $\psi e^{i2\phi_4}$ creates a left-moving electron. For simplicity, we take $\xi_{2\text{LL}}(x)$ as a complex Gaussian random variable: $\langle \xi_{2\text{LL}}(x)\xi^*_{2\text{LL}}(x')\rangle = W_{2\text{LL}}\delta(x - x')$.

We now analyze the influence of $S_{2\text{LL}}$ on the edge transport by considering the linear RG equation for $W_{2\text{LL}}$. From the standard disordered averaged RG scheme [68], we have $d\tilde{W}_{2\text{LL}}/d\ln\ell = (3 - 2\Delta_{2\text{LL}})\tilde{W}_{2\text{LL}}$. Here, ℓ denotes the running length scale, $\Delta_{2\text{LL}}$ is the scaling dimension of $\psi e^{i2\phi_4 + i\phi_3}$, and $\tilde{W}_{2\text{LL}}$ is the dimensionless disorder strength corresponding to $W_{2\text{LL}}$. Hereafter, all appearing dimensionless disorder strengths are denoted with a tilde. When the perturbation (3) is relevant ($\Delta_{2\text{LL}} < 3/2$), the disorder drives the system toward the fixed point $\Delta_{2\text{LL}} = 1$ [14]. The RG flow then introduces an elastic length scale ℓ_0, beyond which disorder mixes the channels within the 2LL. We define ℓ_0 as the scale at which $\tilde{W}_{2\text{LL}}$ is of order unity: $\ell_0 \sim a\tilde{W}^{1/(3-2\Delta_{2\text{LL}})}_{2\text{LL},0}$, where a is the UV length cutoff and $\tilde{W}_{2\text{LL},0} \equiv \tilde{W}_{2\text{LL}}(\ell = a)$. If the edge length L is larger than ℓ_0, the system flows toward the fixed point where it finally decouples into three upstream-propagating neutral Majorana modes ψ_a $(a = 1, 2, 3)$ and three downstream-propagating charge bosonic modes ϕ_1, ϕ_2, and $\phi_\rho = \phi_3 + \phi_4$ [14,15]. In the vicinity of this fixed point, ℓ_0 constitutes the new UV cutoff for the RG analysis below.

We then consider the length ℓ^*_{eq} and its scaling with T, assuming $k_B T \gg eV$, where V is the voltage bias. We first consider low temperature ($T < \tilde{T}$ in Fig. 2). In the vicinity of the fixed point, and in the basis of charged bosons and neutral Majoranas, the part of $S + S_{2\text{LL}}$ equilibrating the 2LL reads

$$S_{\psi\rho} = -\frac{v_{\rho\sigma}}{2\pi}\sum_{a\neq b}\int dxdt\partial_x\phi_\rho\psi_a[R^T(x)L_xR(x)]_{ab}\psi_b.$$

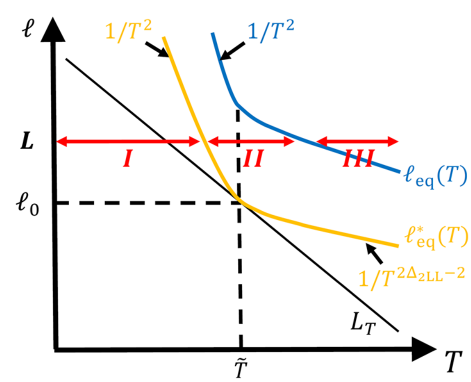

FIG. 2. Schematic log-log plot of the temperature (T) dependence of equilibration lengths ℓ^*_{eq} (within the 2LL) and ℓ_{eq} (between the LLLs and the 2LL) for strong interactions $\Delta_{2\text{LL}} < 3/2$. ℓ_0 is a T-independent elastic length, beyond which channels in the 2LL mix by disorder and the system enters the disorder-dominated phase. $L_T \propto 1/T$ (black thin line) is the thermal length. The scaling of ℓ^*_{eq} and ℓ_{eq} changes at $T = \tilde{T}$, where the transition temperature $\tilde{T}$ is defined as $L_T(\tilde{T}) = \ell_0$. For a given edge length L, three transport regimes $\mathcal{I}$, $\mathcal{II}$, and $\mathcal{III}$ are indicated (see Table I). The voltage V replaces T when $k_B T \ll eV$.

Here, $R(x)$ is a disorder-dependent SO(3) matrix with which the bare action together with Eq. (3) becomes the free-fermion action [14]. Moreover, L_x is the generator of SO(3), describing rotation around the x axis. Under the assumption that $\xi_{\rho\sigma,ab} \equiv v_{\rho\sigma}[R^T(x)L_xR(x)]_{ab}$ is a Gaussian random variable, $\langle \xi_{\rho\sigma,ab}(x)\xi^*_{\rho\sigma,a'b'}(x')\rangle = W_{\rho\sigma,ab}\delta(x-x')\delta_{aa'}\delta_{bb'}$, the disorder strengths $\tilde{W}_{\rho\sigma,ab}$ renormalize according to

$$d\tilde{W}_{\rho\sigma,ab}/d\ln\ell = (3-2\Delta_{\rho\sigma})\tilde{W}_{\rho\sigma,ab} = -\tilde{W}_{\rho\sigma,ab}, \quad (4)$$

since $\Delta_{\rho\sigma} = 2$ (with respect to the disordered fixed point) in the absence of the interactions between the LLLs and the 2LL. When $T < \tilde{T}$, the RG flow in Eq. (4) terminates at the thermal length $L_T \propto 1/T$, where the disorder strengths are

$$\tilde{W}_{\rho\sigma,ab}(L_T) = \tilde{W}^0_{\rho\sigma,ab}\,\ell_0/L_T. \quad (5)$$

Here, $\tilde{W}^0_{\rho\sigma,ab} \equiv \tilde{W}_{\rho\sigma,ab}(\ell_0)$. Below, we focus on $\tilde{W}_{\rho\sigma} \equiv \max[\tilde{W}_{\rho\sigma,ab}]$ as it dominates in equilibrating the 2LL. Beyond L_T, $\tilde{W}_{\rho\sigma}$ scales classically, leading to

$$\tilde{W}_{\rho\sigma}(L_T)/L_T = \tilde{W}_{\rho\sigma}(\ell^*_{\rm eq})/\ell^*_{\rm eq} \sim 1/\ell^*_{\rm eq}, \quad (6)$$

where we defined $\ell^*_{\rm eq}$ as $\tilde{W}_{\rho\sigma}(\ell^*_{\rm eq}) \sim 1$. Combining Eqs. (5) and (6), we obtain the low-temperature scaling

$$\ell^*_{\rm eq} \sim L_T^2/\ell_0\tilde{W}^0_{\rho\sigma} \propto 1/T^2, \quad (7)$$

in agreement with Ref. [69]. For $T > \tilde{T}$ (see Fig. 2), the RG flow terminates at $\ell = L_T$ before reaching the disorder fixed point. A similar RG analysis (see Supplemental Material [70]) results in the high-temperature scaling $\ell^*_{\rm eq} \sim L_T(\ell_0/L_T)^{3-2\Delta_{\rm 2LL}} \propto T^{2-2\Delta_{\rm 2LL}}$. The complete temperature scaling of $\ell^*_{\rm eq}$ is depicted in Fig. 2. The scalings match at the crossover scale $L_T \sim \ell_0 \Leftrightarrow T \sim \tilde{T}$. We now return to the vicinity of the fixed point and consider weak random electron tunneling between edge modes of the LLLs and the 2LL. The perturbing action reads

$$S_{\rm LLM} = \int dtdx e^{i\phi_1(x)}e^{-2i\phi_\rho(x)}\left[\xi_{\rm LLM,1}(x)\left(\frac{\psi_2 - i\psi_3}{2}\right) + \xi_{\rm LLM,2}(x)\left(\frac{\psi_2 + i\psi_3}{2}\right) + \xi_{\rm LLM,3}(x)\psi_1 + \text{H.c.}\right],$$

where $\psi_1 \equiv \psi$, $\psi_2 = e^{i(\phi_3+2\phi_4)} + e^{-i(\phi_3+2\phi_4)}$, and $\psi_3 = -i(e^{i(\phi_3+2\phi_4)} - e^{-i(\phi_3+2\phi_4)})$. We neglect tunneling between ϕ_2 and the 2LL, assuming negligible spin-flip tunneling. With respect to the fixed point, all tunneling operators have scaling dimensions $\Delta_{\rm LLM} = 2$. The disorder strengths are assumed Gaussian: $\langle \xi_{{\rm LLM},i}(x)\xi^*_{{\rm LLM},i'}(x')\rangle = W_{{\rm LLM},i}\delta(x-x')\delta_{ii'}$. The disorder strengths $\tilde{W}_{{\rm LLM},i}$ then renormalize according to

$$d\tilde{W}_{{\rm LLM},i}/d\ln\ell = (3-2\Delta_{\rm LLM})\tilde{W}_{{\rm LLM},i} = -\tilde{W}_{{\rm LLM},i}. \quad (8)$$

Again, we consider only the dominating disorder $\tilde{W}_{\rm LLM} \equiv \max[\tilde{W}_{{\rm LLM},i}]$. Following the procedure leading to Eqs. (5)–(7), we arrive at the length scale $\ell_{\rm eq}$, governing the LLM. It scales as

$$\ell_{\rm eq} \sim L_T^2/\ell_0\tilde{W}^0_{\rm LLM} \propto 1/T^2, \quad (9)$$

where $\tilde{W}^0_{\rm LLM}$ is the disorder strength with the largest value at $\ell = \ell_0$. The low T scaling of $\ell_{\rm eq}$ is depicted in Fig. 2. Our results (7) and (9) imply that $\ell^*_{\rm eq} \ll \ell_{\rm eq}$ (in view of $\tilde{W}^0_{\rm LLM} \ll \tilde{W}^0_{\rho\sigma}$, see Discussion below and Supplemental Material [70]), and thus the transport regime $\mathcal{II}$ holds in a broad temperature window.

Numerical computation of the noise.—Next, we compute the noise scaling using the model from Refs. [58,59]. We introduce a set of virtual reservoirs attached to each channel along the edge. Such reservoirs define and maintain local equilibrium conditions in each channel [56]. In the continuum limit, we obtain a set of transport equations for the local voltages, local temperatures, and the local noise along the edge [70]. By numerically solving these equations for the APF edge, we obtain the plots in Fig. 1. In regime $\mathcal{I}$, S rises first linearly, and then drops exponentially in $L/\ell^*_{\rm eq}$. Around $\log[L/\ell^*_{\rm eq}] \approx 2$ (regime $\mathcal{II}$), $S \simeq c_1 - c_2\sqrt{L/\ell_{\rm eq}}$, with $c_1 \sim 0.1$ and $c_2 \sim 0.01$ [70]. The algebraic corrections to the constant scaling become suppressed for larger $\ell_{\rm eq}$ and develop into a plateau. On this plateau, $G^Q/\kappa T \approx 5/2$. In regime $\mathcal{III}$, $S \simeq e^{-L/\ell^*_{\rm eq}}$ and $G^Q/\kappa T = 3/2$. Figs. 1(d) and 1(e) depict the edge channel temperature profiles in regimes $\mathcal{II}$ and $\mathcal{III}$, respectively. In regime $\mathcal{II}$, heat flows ballistically upstream with diffusive corrections from LLM. In regime $\mathcal{III}$, the upstream heat propagation is exponentially suppressed in L.

Discussion.—We now justify the assumption of weak LLM, i.e., that typical experimental conditions favor regime $\mathcal{II}$. Since ϕ_1 and the 2LL (same spin) are spatially far apart, we assume weak electron tunneling between these levels. By contrast, ϕ_2 and the 2LL are spatially closer, but have opposite spin. Tunneling between them is therefore also strongly suppressed, assuming no (or only weak) spin-rotation symmetry breaking (see Supplemental Material [70]). The detected upstream heat propagation at $\nu = 5/2$ [72] provides further support for regime $\mathcal{II}$.

Our proposed measurement of S should be feasible with present technology. We envision a device capable of measuring both G^Q and $S(L/\ell^*_{\rm eq})$ under no-bulk leakage conditions [34,57]. Measuring $S(L/\ell^*_{\rm eq})$ can be performed either by varying the intercontact distance L, e.g., with a modulation gate, or by using several contacts spaced along the edge. Another possibility is to fix L and instead tune the equilibration length, as was recently demonstrated at $\nu = 2/3$ [73]. Our setup allows, in principle, for observation of a transition of $G^Q/\kappa T$ from 5/2 to 3/2 with increasing L, which would strongly favor the APF state (see Table I).

Summary.—We studied shot noise S on the $\nu = 5/2$ FQH edge for the three main edge candidates consistent with half-integer quantization of G^Q: Pfaffian, particle-hole Pfaffian, and anti-Pfaffian. Assuming full equilibration, which requires strong Landau level mixing, we argued that S vanishes or decays exponentially in the edge length for all three candidates. However, in the regime where Landau level mixing is negligible, but intra-Landau level equilibration is efficient, only the anti-Pfaffian edge generates nonvanishing S. We demonstrated that a transport regime with $G^Q/\kappa T = 5/2$ in combination with $S \simeq c_1 - c_2\sqrt{L/\ell_{\rm eq}}$ uniquely singles out the anti-Pfaffian. By contrast, for the same G^Q, the scaling $S \simeq 0$ points instead strongly toward the particle-hole Pfaffian. The Pfaffian edge exhibits robustly $G^Q/\kappa T = 7/2$ and $S = 0$. We expect our results to be very useful for experimentally determining the $\nu = 5/2$ edge structure. Our analysis can be extended to other mechanisms of partial equilibration (see Supplemental Material [70]) and other FQH states.

We thank A. Stern, Y. Oreg, B. Dutta, R. Melcer, and M. Heiblum for helpful discussions. C. S., Y. G., and A. D. M. acknowledge support by DFG Grant No. MI 658/10-1 and by the German-Israeli Foundation Grant No. I-1505-303.10/2019. Y. G. further acknowledges support by DFG RO 2247/11-1, CRC 183 (project C01), and the Minerva foundation. J. P. acknowledges funding by the Deutsche Forschungsgemeinschaft (DFG, German Research Foundation)—Projektnummer 277101999—TRR 183 (project A01).

J. P. and C. S. contributed equally to this work.

*jinhong@thp.uni-koeln.de
†christian.spanslatt@kit.edu

[1] D. C. Tsui, H. L. Stormer, and A. C. Gossard, Two-Dimensional Magnetotransport in the Extreme Quantum Limit, Phys. Rev. Lett. **48**, 1559 (1982).
[2] R. B. Laughlin, Anomalous Quantum Hall Effect: An Incompressible Quantum Fluid with Fractionally Charged Excitations, Phys. Rev. Lett. **50**, 1395 (1983).
[3] R. Willett, J. P. Eisenstein, H. L. Störmer, D. C. Tsui, A. C. Gossard, and J. H. English, Observation of an Even-Denominator Quantum Number in the Fractional Quantum Hall Effect, Phys. Rev. Lett. **59**, 1776 (1987).
[4] G. Moore and N. Read, Nonabelions in the fractional quantum Hall effect, Nucl. Phys. **B360**, 362 (1991).
[5] E. Fradkin, *Field Theories of Condensed Matter Physics* (Cambridge University Press, Cambridge, England, 2013).
[6] C. Nayak, S. H. Simon, A. Stern, M. Freedman, and S. D. Sarma, Non-Abelian anyons and topological quantum computation, Rev. Mod. Phys. **80**, 1083 (2008).
[7] R. H. Morf, Transition from Quantum Hall to Compressible States in the Second Landau Level: New Light on the $\nu = 5/2$ Enigma, Phys. Rev. Lett. **80**, 1505 (1998).
[8] K. Park, V. Melik-Alaverdian, N. E. Bonesteel, and J. K. Jain, Possibility of p-wave pairing of composite fermions at $\nu = \frac{1}{2}$, Phys. Rev. B **58**, R10167 (1998).
[9] A. E. Feiguin, E. Rezayi, K. Yang, C. Nayak, and S. D. Sarma, Spin polarization of the $\nu = 5/2$ quantum Hall state, Phys. Rev. B **79**, 115322 (2009).
[10] W. Pan, H. Stormer, D. Tsui, L. Pfeiffer, K. Baldwin, and K. West, Experimental evidence for a spin-polarized ground state in the $\nu = 5/2$ fractional quantum Hall effect, Solid State Commun. **119**, 641 (2001).
[11] L. Tiemann, G. Gamez, N. Kumada, and K. Muraki, Unraveling the spin polarization of the $\nu = 5/2$ fractional quantum Hall state, Science **335**, 828 (2012).
[12] M. Stern, B. A. Piot, Y. Vardi, V. Umansky, P. Plochocka, D. K. Maude, and I. Bar-Joseph, Nmr Probing of the Spin Polarization of the $\nu = 5/2$ Quantum Hall State, Phys. Rev. Lett. **108**, 066810 (2012).
[13] J. Biddle, M. R. Peterson, and S. D. Sarma, Variational Monte Carlo study of spin-polarization stability of fractional quantum Hall states against realistic effects in half filled landau levels, Phys. Rev. B **87**, 235134 (2013).
[14] M. Levin, B. I. Halperin, and B. Rosenow, Particle-Hole Symmetry and the Pfaffian State, Phys. Rev. Lett. **99**, 236806 (2007).
[15] S.-S. Lee, S. Ryu, C. Nayak, and M. P. A. Fisher, Particle-Hole Symmetry and the $\nu = \frac{5}{2}$ Quantum Hall State, Phys. Rev. Lett. **99**, 236807 (2007).
[16] L. Fidkowski, X. Chen, and A. Vishwanath, Non-Abelian Topological Order on the Surface of a 3D Topological Superconductor from an Exactly Solved Model, Phys. Rev. X **3**, 041016 (2013).
[17] D. T. Son, Is the Composite Fermion a Dirac Particle?, Phys. Rev. X **5**, 031027 (2015).
[18] P. T. Zucker and D. E. Feldman, Stabilization of the Particle-Hole Pfaffian Order by Landau-Level Mixing and Impurities that Break Particle-Hole Symmetry, Phys. Rev. Lett. **117**, 096802 (2016).
[19] L. Antonić, J. Vučičević, and M. V. Milovanović, Paired states at 5/2: Particle-hole Pfaffian and particle-hole symmetry breaking, Phys. Rev. B **98**, 115107 (2018).
[20] X. G. Wen, Non-Abelian Statistics in the Fractional Quantum Hall States, Phys. Rev. Lett. **66**, 802 (1991).
[21] B. I. Halperin, Theory of the quantized Hall conductance, Helv. Phys. Acta **56**, 75 (1983), https://www.e-periodica.ch/digbib/view?pid=hpa-001:1983:56::1243#87.
[22] G. Yang and D. E. Feldman, Influence of device geometry on tunneling in the $\nu = \frac{5}{2}$ quantum Hall liquid, Phys. Rev. B **88**, 085317 (2013).
[23] G. Yang and D. E. Feldman, Experimental constraints and a possible quantum Hall state at $\nu = 5/2$, Phys. Rev. B **90**, 161306(R) (2014).
[24] M. Storni, R. H. Morf, and S. D. Sarma, Fractional Quantum Hall State at $\nu = 5/2$ and the Moore-Read Pfaffian, Phys. Rev. Lett. **104**, 076803 (2010).
[25] E. H. Rezayi, Landau Level Mixing and the Ground State of the $\nu = 5/2$ Quantum Hall Effect, Phys. Rev. Lett. **119**, 026801 (2017).
[26] I. P. Radu, J. B. Miller, C. M. Marcus, M. A. Kastner, L. N. Pfeiffer, and K. W. West, Quasi-particle properties from

tunneling in the $v = 5/2$ fractional quantum Hall state, Science 320, 899 (2008).
[27] X. Lin, C. Dillard, M. A. Kastner, L. N. Pfeiffer, and K. W. West, Measurements of quasiparticle tunneling in the $\upsilon = \frac{5}{2}$ fractional quantum Hall state, Phys. Rev. B 85, 165321 (2012).
[28] X. Lin, R. Du, and X. Xie, Recent experimental progress of fractional quantum Hall effect: 5/2 filling state and graphene, Natl. Sci. Rev. 1, 564 (2014).
[29] X. G. Wen, Topological orders in rigid states, Int. J. Mod. Phys. B 04, 239 (1990).
[30] X. G. Wen, Chiral Luttinger liquid and the edge excitations in the fractional quantum Hall states, Phys. Rev. B 41, 12838 (1990).
[31] A. M. Chang, Chiral Luttinger liquids at the fractional quantum Hall edge, Rev. Mod. Phys. 75, 1449 (2003).
[32] S. Jezouin, F. D. Parmentier, A. Anthore, U. Gennser, A. Cavanna, Y. Jin, and F. Pierre, Quantum limit of heat flow across a single electronic channel, Science 342, 601 (2013).
[33] M. Banerjee, M. Heiblum, A. Rosenblatt, Y. Oreg, D. E. Feldman, A. Stern, and V. Umansky, Observed quantization of anyonic heat flow, Nature (London) 545, 75 EP (2017).
[34] M. Banerjee, M. Heiblum, V. Umansky, D. E. Feldman, Y. Oreg, and A. Stern, Observation of half-integer thermal hall conductance, Nature (London) 559, 205 (2018).
[35] M. Heiblum and D. Feldman, Edge probes of topological order, Int. J. Mod. Phys. A 35, 2030009 (2020).
[36] C. L. Kane and M. P. A. Fisher, Quantized thermal transport in the fractional quantum Hall effect, Phys. Rev. B 55, 15832 (1997).
[37] A. Cappelli, M. Huerta, and G. R. Zemba, Thermal transport in chiral conformal theories and hierarchical quantum Hall states, Nucl. Phys. B636, 568 (2002).
[38] D. F. Mross, Y. Oreg, A. Stern, G. Margalit, and M. Heiblum, Theory of Disorder-Induced Half-Integer Thermal Hall Conductance, Phys. Rev. Lett. 121, 026801 (2018).
[39] C. Wang, A. Vishwanath, and B. I. Halperin, Topological order from disorder and the quantized Hall thermal metal: Possible applications to the $\nu = 5/2$ state, Phys. Rev. B 98, 045112 (2018).
[40] B. Lian and J. Wang, Theory of the disordered $\nu = \frac{5}{2}$ quantum thermal Hall state: Emergent symmetry and phase diagram, Phys. Rev. B 97, 165124 (2018).
[41] W. Zhu, D. Sheng, and K. Yang, Topological Interface between Pfaffian and Anti-Pfaffian Order in $\nu = 5/2$ Quantum Hall Effect, Phys. Rev. Lett. 125, 146802 (2020).
[42] P.-S. Hsin, Y.-H. Lin, N. M. Paquette, and J. Wang, An effective field theory for fractional quantum Hall systems near $\nu = 5/2$, arXiv:2005.10826.
[43] I. Fulga, Y. Oreg, A. Mirlin, A. Stern, and D. Mross, Temperature enhancement of thermal Hall conductance quantization, arXiv:2006.09392.
[44] S. H. Simon, Interpretation of thermal conductance of the $\nu = 5/2$ edge, Phys. Rev. B 97, 121406(R) (2018).
[45] D. E. Feldman, Comment on "Interpretation of thermal conductance of the $\nu = 5/2$ edge, Phys. Rev. B 98, 167401 (2018).
[46] K. K. W. Ma and D. E. Feldman, Partial equilibration of integer and fractional edge channels in the thermal quantum Hall effect, Phys. Rev. B 99, 085309 (2019).
[47] S. H. Simon and B. Rosenow, Partial Equilibration of the Anti-Pfaffian Edge Due to Majorana Disorder, Phys. Rev. Lett. 124, 126801 (2020).
[48] H. Asasi and M. Mulligan, Partial equilibration of anti-Pfaffian edge modes at $\nu = 5/2$, arXiv:2004.04161.
[49] Y. Blanter and M. Büttiker, Shot noise in mesoscopic conductors, Phys. Rep. 336, 1 (2000).
[50] We consider noise in transport along the edge, distinct from that in tunneling settings [51,52].
[51] M. Carrega, D. Ferraro, A. Braggio, N. Magnoli, and M. Sassetti, Anomalous Charge Tunneling in Fractional Quantum Hall Edge States at a Filling Factor $\nu = 5/2$, Phys. Rev. Lett. 107, 146404 (2011).
[52] M. Carrega, D. Ferraro, A. Braggio, N. Magnoli, and M. Sassetti, Spectral noise for edge states at the filling factor $\nu = 5/2$, New J. Phys. 14, 023017 (2012).
[53] We assume equal heat and charge equilibration lengths even though heat equilibration length may considerably exceed that for charge. Then, our conclusions remain valid with ℓ_{eq} denoting the heat equilibration length.
[54] C. L. Kane and M. P. A. Fisher, Contacts and edge-state equilibration in the fractional quantum Hall effect, Phys. Rev. B 52, 17393 (1995).
[55] I. Protopopov, Y. Gefen, and A. Mirlin, Transport in a disordered $\nu = 2/3$ fractional quantum Hall junction, Ann. Phys. (Amsterdam) 385, 287 (2017).
[56] C. Nosiglia, J. Park, B. Rosenow, and Y. Gefen, Incoherent transport on the $\nu = 2/3$ quantum Hall edge, Phys. Rev. B 98, 115408 (2018).
[57] A. Aharon-Steinberg, Y. Oreg, and A. Stern, Phenomenological theory of heat transport in the fractional quantum Hall effect, Phys. Rev. B 99, 041302(R) (2019).
[58] J. Park, A. D. Mirlin, B. Rosenow, and Y. Gefen, Noise on complex quantum Hall edges: Chiral anomaly and heat diffusion, Phys. Rev. B 99, 161302(R) (2019).
[59] C. Spånslätt, J. Park, Y. Gefen, and A. D. Mirlin, Topological Classification of Shot Noise on Fractional Quantum Hall Edges, Phys. Rev. Lett. 123, 137701 (2019).
[60] C. Spånslätt, J. Park, Y. Gefen, and A. D. Mirlin, Conductance plateaus and shot noise in fractional quantum Hall point contacts, Phys. Rev. B 101, 075308 (2020).
[61] Equilibration between channels in the LLLs is immaterial since they both propagate downstream.
[62] Possible edge reconstruction [63–65] does not change ν_Q and only transforms $S = 0$ into $S \sim \exp(-L/\ell^*_{\mathrm{eq}}) \simeq 0$.
[63] X. Wan, K. Yang, and E. H. Rezayi, Edge Excitations and Non-Abelian Statistics in the Moore-Read State: A Numerical Study in the Presence of Coulomb Interaction and Edge Confinement, Phys. Rev. Lett. 97, 256804 (2006).
[64] X. Wan, Z.-X. Hu, E. H. Rezayi, and K. Yang, Fractional quantum Hall effect at $\nu = 5/2$: Ground states, non-Abelian quasiholes, and edge modes in a microscopic model, Phys. Rev. B 77, 165316 (2008).
[65] Y. Zhang, Y.-H. Wu, J. A. Hutasoit, and J. K. Jain, Theoretical investigation of edge reconstruction in the $\nu = 5/2$ and 7/3 fractional quantum Hall states, Phys. Rev. B 90, 165104 (2014).
[66] J. Park, B. Rosenow, and Y. Gefen, Symmetry-related transport on a fractional quantum Hall edge, arXiv:2003.13727.

[67] C. L. Kane, M. P. A. Fisher, and J. Polchinski, Randomness at the Edge: Theory of Quantum Hall Transport at Filling $\nu = 2/3$, Phys. Rev. Lett. **72**, 4129 (1994).
[68] T. Giamarchi and H. J. Schulz, Anderson localization and interactions in one-dimensional metals, Phys. Rev. B **37**, 325 (1988).
[69] K. K. Ma and D. Feldman, Thermal Equilibration on the Edges of Topological Liquids, Phys. Rev. Lett. **125**, 016801 (2020).
[70] See Supplemental Material at http://link.aps.org/supplemental/10.1103/PhysRevLett.125.157702 for details on RG calculations, numerical computation of equilibration and noise on the APF edge, estimates of parameters, and comparison to alternative mechanisms of partial equilibration, which includes Ref. [71].
[71] Y. Gross, M. Dolev, M. Heiblum, V. Umansky, and D. Mahalu, Upstream Neutral Modes in the Fractional Quantum Hall Effect Regime: Heat Waves or Coherent Dipoles, Phys. Rev. Lett. **108**, 226801 (2012).
[72] A. Bid, N. Ofek, H. Inoue, M. Heiblum, C. L. Kane, V. Umansky, and D. Mahalu, Observation of neutral modes in the fractional quantum Hall regime, Nature (London) **466**, 585 (2010).
[73] Y. Cohen, Y. Ronen, W. Yang, D. Banitt, J. Park, M. Heiblum, A. D. Mirlin, Y. Gefen, and V. Umansky, Synthesizing a $\nu = 2/3$ fractional quantum Hall effect edge state from counter-propagating $\nu = 1$ and $\nu = 1/3$ states, Nat. Commun. **10**, 1920 (2019).